

The above matrix can be found by using the form for the general momentum matrices found by Slonczewski. From that work we have an important result: all of the subgroups possible at a general point on the zone edge are included in the four bands. This means that when (2.2) is treated exactly, it includes effects of the type represented by (A.2). Let us illustrate this statement. Suppose that we are dealing with a case in which  $E_1$ ,  $E_2$ , and  $E_3$  are all different. Further, suppose that we are interested only in the two bands derived from 31 and 32, so that we may eliminate bands 1 and 2 by perturbation theory. We would then find in our two-band sub-Hamiltonian terms like those given by  $D_{33}$  in Eq. (A.2). The same kind of argument holds if we eliminate bands 31 and 32 and keep bands 1 and 2. Of course, if  $E_1$  or  $E_2$  is equal to  $E_3$ , we cannot use pertur-

bation theory, but the *type* of interaction does not change. As the differences between  $E_1$  or  $E_2$  and  $E_3$  are of the order of tenths of electron volts, and as the nearest state in energy to the four bands of interest is several electron volts away, the effect of the terms in (A.2) must be small compared to those already present in (2.2).

Still higher terms could contribute. For example, the fourth-order terms produce the analog to the free-atom diamagnetism. We will not give a complete discussion of the higher terms. However, we have shown that the second-order terms are negligible, and the order of magnitude of the fourth-order terms is probably of the order of the free-atom diamagnetism, which is small ( $0.5 \times 10^{-6}$  emu/g).

PHYSICAL REVIEW

VOLUME 119, NUMBER 2

JULY 15, 1960

## Infrared Absorption and Valence Band in Indium Antimonide\*

G. W. GOBEL† AND H. Y. FAN  
Purdue University, Lafayette, Indiana

(Received March 14, 1960)

Infrared absorption is studied at near liquid helium temperature for *n*- and *p*-type degenerate samples of various carrier concentrations. The absorption in *p*-type samples, at photon energies larger than the energy gap, depends on the hole concentration. The results show that the valence band is warped and that the energy at  $k=0$  is very close to the maximum energy of the band. A step in the absorption of *n*-type samples is observed which gives an estimate of  $\sim 0.012m$  for the effective mass of light holes. The long wavelength absorption in *p*-type samples is characteristic of intervalence band transitions.

### INTRODUCTION

INFRARED studies of indium antimonide have contributed a large amount of experimental information about the conduction band which is consistent with a model of an energy minimum at the center of the Brillouin zone and an effective mass varying with energy. Observations of a change of absorption edge with the concentration of conduction electrons<sup>1,2</sup> gave a rough estimate of the effective mass for the conduction band. Consistent values of the effective mass have been obtained from various types of experiments including cyclotron resonance,<sup>3</sup> reflection and absorption at long wavelengths,<sup>4</sup> Faraday rotation,<sup>5</sup> and magneto-oscil-

latory effect.<sup>6</sup> The reflection and absorption studies made on samples of various carrier concentrations explored a considerable range of the conduction band, giving the variation of effective mass with energy. The magneto-oscillatory effect experiments gave an estimate of the gyromagnetic ratio for the conduction electrons.

Experimental information about the valence band, including the results of infrared studies, is not as conclusive, as uncertainty is involved in the interpretation of some of the observations. Theoretical treatments suggest that the valence band resembles to some extent that of germanium and silicon but that there may be a number of energy maxima due to the lack of the center of symmetry.<sup>7,8</sup> Estimates of the effective mass for holes, varying from  $0.1m$  to  $0.2m$ , have been deduced from different types of measurements;<sup>4,9</sup> for a complicated band structure, masses obtained from different

\* Work supported by a Signal Corps contract.

† Now at Bell Telephone Laboratories, Murray Hill, New Jersey.

<sup>1</sup> H. J. Hrostowski, G. H. Wheatley, and W. F. Flood, Jr., *Phys. Rev.* **95**, 1683 (1954); E. Burstein, *Phys. Rev.* **93**, 632 (1954); R. G. Breckenridge, R. F. Blunt, W. R. Hosler, H. P. R. Frederikse, J. H. Becker, and W. Oshinsky, *Phys. Rev.* **96**, 571 (1954).

<sup>2</sup> W. Kaiser and H. Y. Fan, *Phys. Rev.* **98**, 966 (1955).

<sup>3</sup> E. Burstein, G. S. Picus, and H. A. Gebbie, *Phys. Rev.* **103**, 825 (1956); R. J. Keyes, S. Zwerdling, S. Foner, H. H. Kolm, and B. Lax, *Phys. Rev.* **104**, 1804 (1956).

<sup>4</sup> W. G. Spitzer and H. Y. Fan, *Phys. Rev.* **106**, 882 (1957).

<sup>5</sup> T. S. Moss, S. D. Smith, and K. W. Taylor, *J. Phys. Chem. Solids* **8**, 323 (1959).

<sup>6</sup> E. Burstein and G. S. Picus, *Phys. Rev.* **105**, 1123 (1957); S. Zwerdling, B. Lax, and L. M. Roth, *Phys. Rev.* **108**, 1402 (1957); E. Burstein, G. S. Picus, R. F. Wallis, and F. Blatt, *Phys. Rev.* **113**, 15 (1959); L. M. Roth, B. Lax, and S. Zwerdling, *Phys. Rev.* **114**, 90 (1959).

<sup>7</sup> G. Dresslhaus, *Phys. Rev.* **100**, 580 (1955); R. H. Parmenter, *Phys. Rev.* **100**, 573 (1955).

<sup>8</sup> E. O. Kane, *J. Phys. Chem. Solids* **1**, 249 (1957).

types of experiments do not have the same significance and are not basic parameters characterizing the band structure. Some indication of the existence of light holes was obtained from the measurements of the variation of Hall coefficient and magnetoresistance with magnetic field<sup>9,10</sup> and from infrared absorption of *p*-type samples at long wavelengths.<sup>2,11</sup> Observed infrared absorption near the intrinsic edge has been attributed to indirect transitions,<sup>11,12</sup> and it has been suggested on this basis that the valence band has maxima far from the center of the Brillouin zone.<sup>13</sup> On the other hand, it has been shown<sup>11,14</sup> that, with a maximum of the valence band at the same point of *k* space as the minimum of the conduction band, there may still be indirect transitions accounting for the observation. Regarding this point, deductions from the piezoresistance measurements are also uncertain. Similar observations have been interpreted as evidence for off-center maxima<sup>15</sup> as well as being consistent with a band structure similar to that of germanium and silicon.<sup>16</sup> It has been also suggested<sup>9</sup> on the basis of large ratios of transverse to longitudinal magnetoresistance for both  $\langle 100 \rangle$  and  $\langle 110 \rangle$  directions that the valence band is isotropic or that it has several maxima with nearly spherical surfaces of constant energy. However, the magnetoresistance ratios for the two directions are fairly large also in the case of *p*-type germanium and silicon, and even larger ratios were given by calculations based on the warped valence bands.<sup>17</sup>

Our measurements of infrared absorption in samples of low carrier concentrations showed that the spectral variation of absorption above the absorption level of  $\sim 500 \text{ cm}^{-1}$ , is consistent with that of direct transitions.<sup>18</sup> Over the range from liquid nitrogen to room temperature, the threshold can be expressed as a constant term  $E_0$ , plus a term linear in temperature. The value of  $E_0$  is close to the value obtained from the intrinsic Hall coefficient and resistivity, indicating that the maximum of the valence band is near  $k=0$ . In the work reported here,<sup>19</sup> absorption was studied for *n*- and *p*-type samples near liquid helium temperature. Samples of various carrier concentrations were used which were degenerate at the low temperature. Absorption was measured to

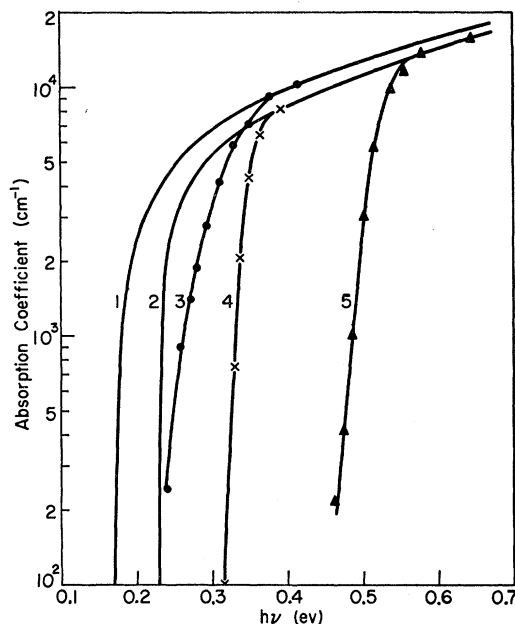


FIG. 1. Absorption edge in pure and *n*-type degenerate samples. Curves 1 and 2 are for pure samples at room temperature and liquid nitrogen temperature, respectively. Curves 3 and 4 show the absorption at the two temperatures for a sample having  $6.1 \times 10^{17} \text{ cm}^{-3}$  carriers. Curve 5 shows the absorption at  $\sim 5^\circ \text{K}$  in a sample having  $2.3 \times 10^{18} \text{ cm}^{-3}$  carriers.

photon energies much higher than the energy gap. Measurements on *p*-type samples were extended also to long wavelengths. Analyses of the results showed that heavy hole band is warped and multiple maxima, if present, are not very pronounced. An estimate of the effective mass of the light hole band was also obtained.

#### ABSORPTION EDGE OF *P*-TYPE SAMPLES

We shall first consider briefly the effect of degenerate carriers in *n*-type samples. The absorption of pure samples is shown by curves 1 and 2, Fig. 1, for room temperature and liquid nitrogen temperature, respectively. Curves 3 and 4 give the absorption at the two temperatures for an *n*-type sample with an electron concentration of  $6.1 \times 10^{17} \text{ cm}^{-3}$ . The absorption edge shifts to larger photon energies as a result of the filling of the low-lying energy levels by the conduction electrons. Curve 4 for liquid nitrogen temperature is steeper than curve 3 for room temperature. The phenomenon can be understood on the basis that the drop of electron occupation at the Fermi level has more straggling at higher temperatures. The following relation can be easily derived on this basis:<sup>2</sup>

$$h\nu + (1 + \epsilon_v/\epsilon_c)kT \ln(\alpha_0/\alpha - 1) = E_G + (1 + \epsilon_c/\epsilon_v)\epsilon_c(\zeta) \quad (1)$$

where  $E_G$  is the energy gap,  $\alpha$  and  $\alpha_0$  are the absorption coefficients at the frequency  $\nu$  for the *n*-type sample and the pure sample, respectively,  $\epsilon_v/\epsilon_c$  is the ratio of en-

<sup>9</sup> H. P. R. Frederikse and W. R. Hosler, Phys. Rev. **108**, (1957); references are given to various mass determinations.

<sup>10</sup> H. J. Hrostowski, F. J. Morin, T. H. Geballe, and G. H. Wheatley, Phys. Rev. **100**, 1672 (1955); C. H. Champness, Phys. Rev. Letters **1**, 433 (1958).

<sup>11</sup> S. W. Kurnick and J. M. Powell, Phys. Rev. **116**, 597 (1959).

<sup>12</sup> V. Roberts and G. E. Quarrington, J. Elect. **1**, 152 (1955).

<sup>13</sup> E. Blount, J. Callaway, M. Cohen, W. Dumke, and J. Phillips, Phys. Rev. **101**, 563 (1956).

<sup>14</sup> W. P. Dumke, Phys. Rev. **108**, 1419 (1957).

<sup>15</sup> R. W. Keyes, Phys. Rev. **99**, 490 (1955); A. J. Tuzzolino, Phys. Rev. **105**, 1411 (1957).

<sup>16</sup> R. F. Potter, Phys. Rev. **108**, 652 (1957).

<sup>17</sup> J. G. Mavroides and B. Lax, Phys. Rev. **107**, 1530 (1957).

<sup>18</sup> H. Y. Fan and G. W. Gobeli, Bull. Am. Phys. Soc. **1**, 111 (1956); H. Y. Fan, Repts. Progr. in Phys. **16**, 107 (1956); see also reference 8.

<sup>19</sup> G. W. Gobeli and H. Y. Fan, Bull. Am. Phys. Soc. **2**, 121 (1957).

ergies in the valence band and the conduction band for a given wave number  $k$ , and  $\epsilon_c(\zeta)$  is the value of  $\epsilon_c$  corresponding to the Fermi level  $\zeta$ . Absorption curves measured on various samples at room temperature and liquid nitrogen temperature can be fitted reasonably well with this relation. Since the effective mass of electrons is known to be much smaller than that of the holes, the ratio  $\epsilon_v/\epsilon_c$  is small, and a value of 0.1 has been assumed. Figure 2 shows the curve of  $\epsilon_c$  as a function of the wave number according to Spitzer and Fan.<sup>4</sup> Since the carrier concentration and the wave number of the Fermi surface have a one to one correspondence, this curve gives also  $\epsilon_c(\zeta)$  as a function of the carrier concentration. The points in Fig. 2 are obtained from the absorption edge measured on samples of various carrier concentrations. They are seen to be in good agreement with the curve.

Curve 5, Fig. 1, gives the results obtained on a sample near liquid helium temperature. The curve and similar results obtained on other samples can not be fitted with Eq. (1), according to which the absorption edge should have been much steeper. We shall return to this point later. Since the absorption edge at liquid nitrogen temperature as represented by curve 4 has a slope comparable to that observed at the low temperature, the application of Eq. (1) to the data for liquid nitrogen temperature is questionable and the estimate of  $\epsilon_c(\zeta)$  is therefore subject to some uncertainty. This difficulty is less important for the room temperature results.

We turn now to  $p$ -type samples. If the valence band had only one branch and if the absorption were produced by direct transitions, then the absorption edge of a degenerate  $p$ -type sample should be the same as that of a degenerate  $n$ -type sample having the same carrier concentration. This follows from the fact that the carrier concentration (C.C.) is directly related to the volume,  $V_k(\zeta)$ , of wave-number space bound by the Fermi surface, i.e.

$$\text{C.C.} = 2V_k(\zeta) = 2(4\pi/3)k^3 \quad (2)$$

in the case of a energy band having spherical constant-energy surfaces centered at  $k=0$ . Thus an  $n$ -type or a  $p$ -type sample having a given carrier concentration will have energy levels in the conduction band or the valence band filled by carriers up to the same  $k$ , ruling out transitions for smaller wave numbers.

Figure 3 shows some of the experimental results for  $p$ -type samples. In general, the absorption departs from the curve for pure samples at a frequency about as expected for an  $n$ -type sample. However, the absorption decreases gradually and extends to an absorption edge at about the same position as in pure samples, in striking contrast with the case of  $n$ -type samples shown in Fig. 1. The explanation for the difference between  $n$ - and  $p$ -type samples is to be found in the structure of the valence band.

Figure 4 shows schematically the energy band structure with the valence band consisting of three branches

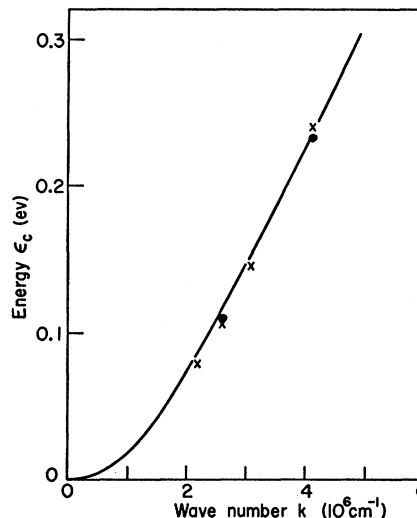


FIG. 2. Energy as a function of wave number for the conduction band. The curve is essentially that given by Spitzer and Fan.<sup>4</sup> The points are obtained from estimates of Fermi energy based on the absorption edge of degenerate  $n$ -type samples: the dots are obtained from room temperature data and the crosses are based on data for 78°K.

$V_1$ ,  $V_2$ , and  $V_3$ , each doubly degenerate. The heavy hole band,  $V_1$ , may actually be split and have several maxima instead of one maximum at  $k=0$ . However, as pointed out in the introduction, we believe that the maximum energy of the valence band occurs in the neighborhood of  $k=0$ . Furthermore, it will be seen later that multiple maxima, if present, can not be very pronounced.

In a  $p$ -type degenerate sample, in which the energy levels above the Fermi level  $\zeta$  are occupied by holes, optical transitions from  $V_1$  to the conduction band are ruled out for frequencies smaller than  $h\nu_1$ . However, transitions from  $V_2$  to the conduction band are possible down to  $h\nu_2$ . With a  $V_2$  band having a large curvature,  $h\nu_2$  may be close to the energy gap in magnitude. Hence, transitions from the  $V_2$  band could give an absorption persisting to the neighborhood of the absorption edge in pure samples. Thus, the existence of the  $V_2$  band seems to explain qualitatively the failure of the absorption to cut off sharply as in  $n$ -type samples. The absorption is expected, however, to show a steep drop at  $h\nu_1$  due to the cutoff of transitions from the  $V_1$  band. Experimentally, the absorption does not show a stepwise drop, instead the absorption falls off gradually from the absorption of pure samples. The discrepancy between the expected and the observed behaviors becomes clear from the following considerations. The hole distribution in the  $V_1$  band falls off within a range of a few  $kT$  around the Fermi level. The photon energy for optical transition is given by

$$h\nu = E_G + \epsilon_{v1} + \epsilon_3 \quad (3)$$

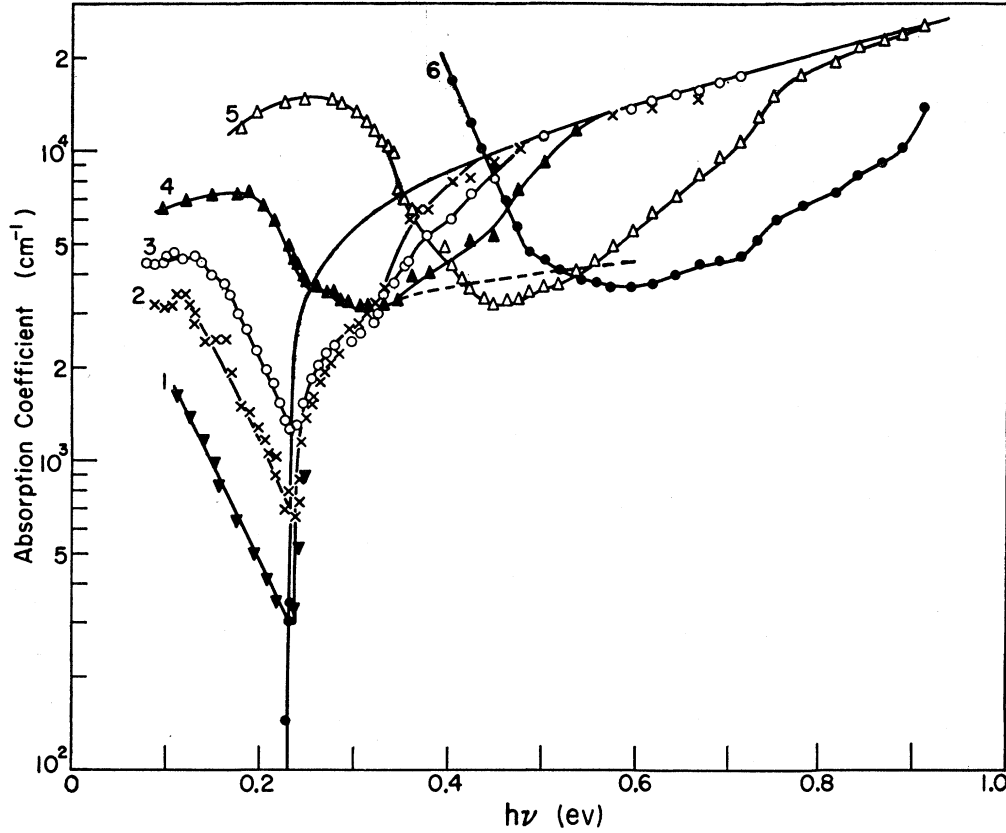


FIG. 3. Absorption coefficient at  $\sim 5^\circ\text{K}$  as a function of photon energy for degenerate  $p$ -type samples. The carrier concentrations in units of  $\text{cm}^{-3}$  are:

- 1,  $5.5 \times 10^{17}$ ;
- 2,  $9.0 \times 10^{17}$ ;
- 3,  $1.56 \times 10^{18}$ ;
- 4,  $2.6 \times 10^{18}$ ;
- 5,  $9.4 \times 10^{18}$ ;
- 6,  $2.0 \times 10^{19}$ .

where  $E_G$  is the energy gap,

$$\epsilon_{v1} = \hbar^2 k^2 / 2m_{v1}, \quad \epsilon_c = \hbar^2 k^2 / 2m_c.$$

An energy spread  $\delta\epsilon_{v1}$  is magnified by a factor  $(1+m_{v1}/m_c)$  in the spread  $\delta(h\nu)$  photon energy. Assuming the ratio of effective masses to be  $\sim 10$ , the absorption should drop from its full magnitude to less than 10% over a range of  $\delta(h\nu) \sim 40kT$ . For  $T \sim 5^\circ\text{K}$ ,  $\delta(h\nu) \sim 0.017$  eV. Fig. 3 shows, however, that the difference between the absorption of a  $p$ -type sample and the absorption of pure samples increases much more gradually, reaching a maximum over a range of  $> 0.1$  eV in photon energy. Therefore, the temperature straggling of hole distribution at the Fermi level is far from adequate to explain the gradual decrease of absorption.

We interpret the gradual decrease of the absorption as an indication of a warping of the  $V_1$  band. The energy in the  $V_1$  band may be approximated by an expression of the following form:<sup>8</sup>

$$\epsilon_{v1} = \alpha k^2 [1 - \gamma (k_x^2 k_y^2 + k_y^2 k_z^2 + k_z^2 k_x^2) / k^4], \quad (4)$$

where  $x, y, z$  directions are taken along the cubic axes of the crystal. The parameter  $\gamma$  introduces a warping of the constant energy surfaces, making them non-spherical. The energy varies as  $\alpha k^2$  along the direction of a cubic axis while varying as  $\alpha(1-\gamma/3)k^2$  along the direction of a body diagonal. The situation is shown

schematically in Fig. 5. With holes filling the energy levels above  $\zeta$ , direct transitions from  $V_1$  to the conduction band is eliminated for  $h\nu < h\nu_1'$ . Transitions for  $h\nu > h\nu_1$  are not affected by the holes. In the range  $h\nu_1' < h\nu < h\nu_1$ , the transitions are partially eliminated by the presence of holes. Thus, the absorption associated with the transitions begins at  $h\nu_1'$  but does not reach the full possible magnitude until  $h\nu_1$ .

The optical absorption coefficient is given by the usual expression:

$$\alpha = \frac{4\pi}{cn} \frac{e^2}{6m^2 h\nu} |\bar{p}|^2 \rho(\nu) \propto |\bar{p}|^2 \frac{\rho(\nu)}{\nu}, \quad (5)$$

where  $n$  is the refractive index,  $|\bar{p}|^2/3$  is the square of the momentum matrix element averaged over directions, and  $\rho(\nu)d\nu$  is the number of states in either band for which the transition frequency lies between  $\nu$  and  $\nu+d\nu$ .

$$\rho(\nu) = \frac{2h}{(2\pi)^3} \frac{dV_k(h\nu)}{d(h\nu)} = \frac{2h}{(2\pi)^3} V_k', \quad (6)$$

where  $V_k(h\nu)$  is the volume in  $\vec{k}$  space bound by the surface of transition frequency  $\nu$ . The transition frequency is given by (3) where  $\epsilon_{v1}$  is given by (4). Since  $\epsilon_{v1}$  is much smaller than either  $\epsilon_c$  or  $E_G$  it is a reasonable

approximation to treat the ratio,  $\epsilon_{v1}/\epsilon_c$ , as a constant. We have then:

$$h\nu \approx E_G + (1 + \epsilon_{v1}/\epsilon_c)\epsilon_c \quad (7)$$

and

$$V_k' = \int \frac{ds}{|\text{grad}_k h\nu|} = (1 + \epsilon_{v1}/\epsilon_c)^{-1} \int \frac{ds}{|\text{grad}_k \epsilon_c|}, \quad (8)$$

where  $ds$  is an element of surface of constant  $h\nu$  or  $\epsilon_c$ . In the conduction band of indium antimonide,  $\epsilon_c$  depends only on the magnitude of the wave number. Therefore, we can write:

$$\rho(\nu) \propto \left[ \frac{k^2}{|\text{grad}_k \epsilon_c|} \right]_{h\nu} \int \sin\theta d\theta d\phi. \quad (9)$$

If the conduction band could be characterized by a constant effective mass,  $|\text{grad}_k \epsilon_c|$  would be proportional to  $k$  and  $\rho(\nu)$  would be proportional to  $\sqrt{\epsilon_c}$ . This is not true, however, for the conduction band of indium antimonide. We shall obtain the value of  $|\text{grad}_k \epsilon_c|$  from the curve  $\epsilon_c(k)$  given in Fig. 2.

We are interested in calculating the absorption which is eliminated by the presence of holes in the  $V_1$  band. All transitions for  $h\nu < h\nu_1'$  involve states occupied by the holes, therefore the integration in (9) should extend over the full range:  $0 \leq \theta \leq \pi$  and  $0 \leq \phi \leq 2\pi$ . For  $h\nu > h\nu_1'$ , the range of integration is limited by the intersection of the surface of constant  $h\nu$  with the Fermi surface in  $V_1$  band. It follows from (4) that the range is determined by the condition:

$$\alpha k^2 [1 - \gamma(k_x^2 k_y^2 + k_y^2 k_z^2 + k_z^2 k_x^2)/k^4] \leq \epsilon_{v1}(\zeta), \quad (10)$$

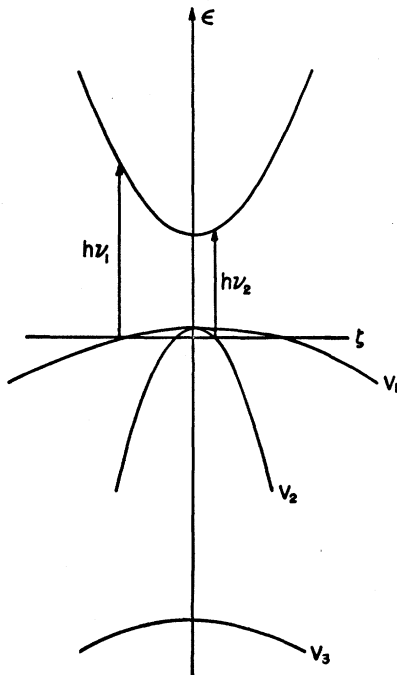


FIG. 4. Schematic diagram of energy bands of indium antimonide.

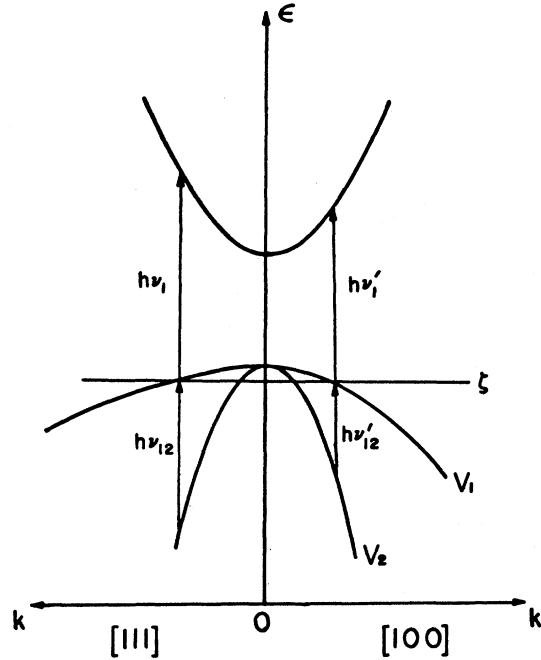


FIG. 5. Schematic diagram of energy bands showing a warped  $V_1$  band and the Fermi level  $\zeta$  of a degenerate  $p$ -type sample.

where the value of  $k$  for a given  $h\nu$  is determined from the curve  $\epsilon_c(k)$  for the value  $\epsilon_c = (h\nu - E_G)/(1 + \epsilon_{v1}/\epsilon_c)$ . It has been suggested that the maximum energy of the  $V_1$  band may occur in the  $\langle 111 \rangle$  directions. We assume therefore that  $\gamma$  is positive, i.e., the constant energy surfaces bulge in  $\langle 111 \rangle$  directions. We have then for  $h\nu_1' < h\nu < h\nu_1$ :

$$\int \sin\theta d\theta d\phi = 4 \int \sin\theta \left[ \frac{\pi}{2} - \sin^{-1} \left( \frac{C - \sin^2 2\theta}{\sin^4 \theta} \right) \right] d\theta, \quad (11)$$

where

$$C = \frac{4}{\gamma} \left[ 1 - \frac{\epsilon_{v1}(\zeta)}{\alpha k^2} \right] = \frac{4}{\gamma} \left[ 1 - \left( \frac{k_1'}{k} \right)^2 \right],$$

$k_1'$  being the wave number corresponding to  $h\nu_1'$ . The limits of integration in (11) are determined by:

$$\frac{1}{3} [2 - (4 - 3C)^{1/2}] \leq \sin^2 \theta \leq \frac{1}{3} [2 + (4 - 3C)^{1/2}]. \quad (12)$$

The maximum photon energy,  $h\nu_1$ , is related to  $h\nu_1'$  through the corresponding wave numbers  $k_1$  and  $k_1'$ :

$$k_1' = k_1 (1 - \gamma/3)^{1/2}.$$

The full absorption for  $V_1$ -conduction band transitions can be calculated as a function of  $h\nu$  by using (5) and (9). The magnitude of the absorption is adjusted so as to obtain a lower envelope for the absorption curves of the various  $p$ -type samples by subtracting the calculated absorption from the absorption of pure samples. The envelope curve obtained is shown by curve A in Fig. 6 and by the dashed curve in Fig. 3. The

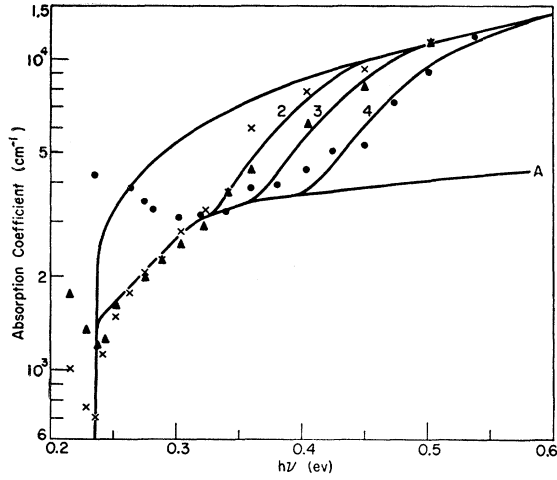


FIG. 6. Absorption coefficient as a function of photon energy for *p*-type samples 2, 3, and 4. Curves 2, 3, and 4 are calculated for  $h\nu_1' = 0.325, 0.355, \text{ and } 0.395 \text{ eV}$ , respectively. Curve A corresponds to the case of a  $V_1$  band filled with holes.

absorption of the samples of two highest carrier concentrations falls somewhat below the curve. This does not seem to be serious in view of the experimental accuracy and possible complications involved in going to large  $h\nu$  and high-impurity concentrations. Depending upon the carrier concentration, the absorption in a given sample should depart from the envelope curve at the appropriate photon energy  $h\nu_1'$  and merge with the absorption curve of pure samples at corresponding  $h\nu_1$ . The absorption between  $h\nu_1'$  and  $h\nu_1$  can be calculated by using (11) instead of (9). Curves 2, 3, 4 in Fig. 6 are calculated in the attempt to fit the experimental data of samples 2, 3, and 4. Each curve was calculated for a chosen value of  $h\nu_1'$ . The three values of  $h\nu_1'$  were chosen so as to satisfy the requirement that the values of  $k$  corresponding to  $\epsilon_c = (h\nu_1' - E_G)/(1 + \epsilon_0/\epsilon_c)$  should be proportional to the one-third power of the carrier concentration. A value of  $\gamma = 2$  was used which seems to give the best fit. Taking into account that in these calculations use has to be made of the  $\epsilon_c(k)$  curve obtained from an entirely different type of experiment and considering the accuracy of the experimental points, the fit obtained is quite satisfactory.

An effective density-of-states mass may be defined by the equation:

$$2\pi(2m_d/\hbar^2)^{3/2}\epsilon^{1/2} = dV_k(\epsilon)/d\epsilon. \quad (13)$$

The energy expression (4) for the  $V_1$  band gives

$$V_k(\epsilon) = (4\pi/3)(\epsilon/\alpha)^{3/2}A, \quad (14)$$

where

$$A = -\int_0^{\pi/2} \sin\theta d\theta \int_0^{\pi/2} \left[ 1 - \frac{\gamma}{4}(\sin^2 2\theta + \sin^4 \theta \sin^2 2\phi) \right]^{3/2} d\phi.$$

We define  $m_1'$  and  $m_1$  by

$$\hbar^2/2m_1' = \alpha, \quad \hbar^2/2m_1 = \alpha(1 - \gamma/3). \quad (15)$$

These quantities may be thought of as effective masses along the  $\langle 100 \rangle$  and  $\langle 111 \rangle$  directions, respectively. Using the value  $\gamma = 2$  obtained above, we got

$$m_1/m_1' = 3, \quad m_d/m_1' = 1.84. \quad (16)$$

According to (13) the volume,  $V_k(\zeta)$ , bound by the Fermi surface can be written:

$$V_k(\zeta) = \frac{4\pi}{3} \left( \frac{2m_d}{\hbar^2} \zeta \right)^{3/2} = \frac{4\pi}{3} \left( \frac{2m_d}{\hbar^2} \frac{\hbar^2}{2m_1'} k_1' \right)^{3/2} = \frac{4\pi}{3} \left( \frac{m_d}{m_1'} k_1' \right)^{3/2}, \quad (17)$$

where  $k_1'$  is the wave number of the Fermi surface along the  $\langle 100 \rangle$  directions and is associated with  $h\nu_1'$ . Since  $V_k(\zeta)$  is related to the carrier concentration by (2), (17) can be used to determine the value of  $k_1'$  and hence the value of  $h\nu_1'$  for a given carrier concentration, once  $m_d/m_1'$  is known. For the value of  $m_d/m_1'$  obtained, the values of  $h\nu_1'$  used in calculating the curves 2, 3, and 4 correspond to carrier concentrations within 10% of the measured carrier concentrations of the samples 2, 3, and 4, respectively. This agreement is a check in comparing the data with the calculated curves.

Since the effective mass of holes in the  $V_1$  band must be much larger than the effective mass of electrons, the threshold for direct transitions should correspond to  $k=0$  even if the valence band had multiple maxima occurring off the center. Therefore, a degenerate *p*-type

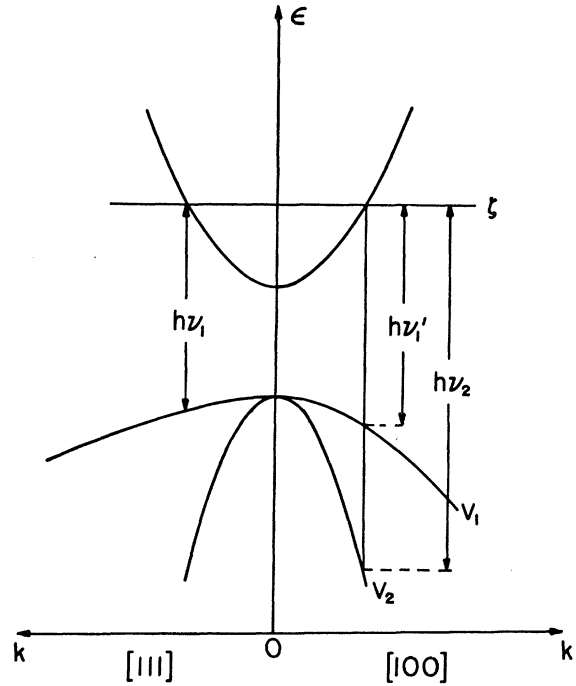


FIG. 7. Schematic diagram of energy bands showing a warped  $V_1$  band and the Fermi level  $\zeta$  of a degenerate *n*-type sample.

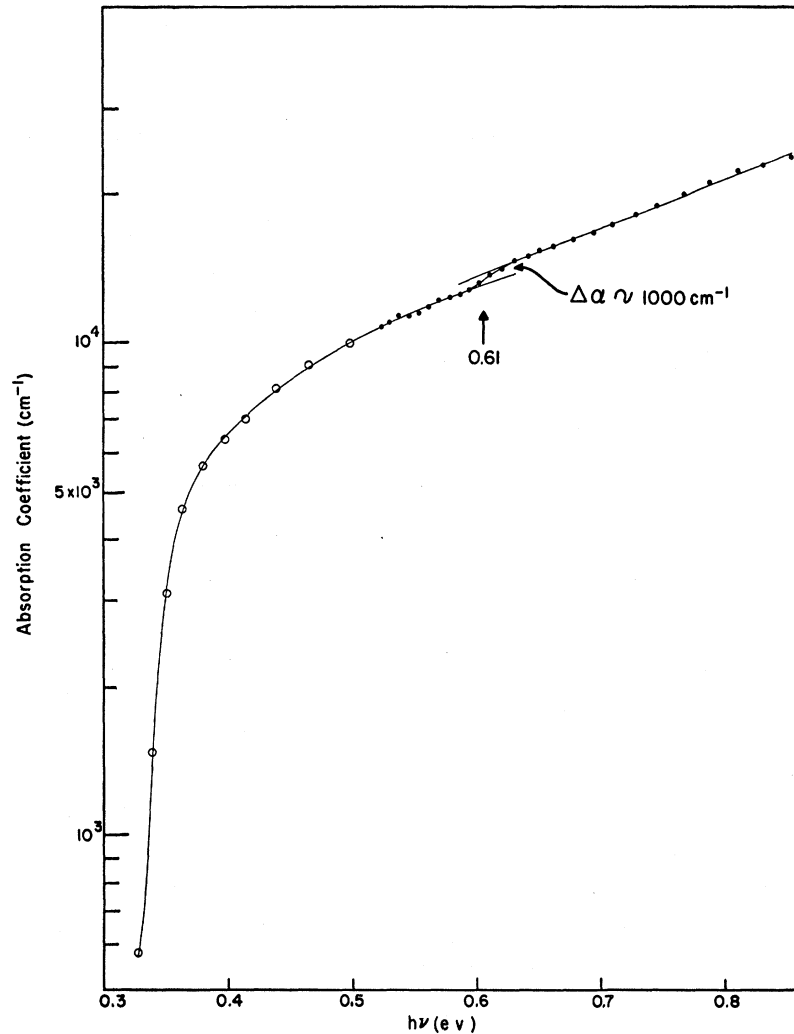


FIG. 8. Absorption coefficient as a function of photon energy for an  $n$ -type sample of  $6.6 \times 10^{17} \text{ cm}^{-3}$  carrier concentration.

with a Fermi level below the maxima but above the point at  $k=0$  would show full absorption near the threshold with a deficiency in absorption beginning at a somewhat higher energy. The fact that such behavior was not observed even for sample 1 of the smallest carrier concentration shows that the maxima can not be very pronounced. The sample has a hole concentration of  $5.5 \times 10^{17} \text{ cm}^{-3}$ . Assuming an effective density-of-states mass of  $0.18m$ , the Fermi level in the sample should be about  $1.35 \times 10^{-2} \text{ eV}$  below the maximum energy of the band. If the energy at  $k=0$  is below the maximum energy of the band by a larger amount, full absorption would have been observed near the threshold.

#### ABSORPTION IN $N$ -TYPE SAMPLES

Referring to Fig. 7. Direct transitions from  $V_1$  to the conduction band begin at photon energy  $h\nu_1$  and reach quickly the full value as in pure samples at  $h\nu_1'$ . The absorption rises steeply in this region, giving the absorption edge. However, direct transitions from the  $V_2$

band do not come in until a higher photon energy,  $h\nu_2$ , is reached. Thus the existence of the  $V_2$  band leads us to expect another rise of absorption at some frequency considerably higher than the threshold. Observation of the effect requires very thin samples since the absorption coefficient increases with frequency. Figure 8 shows the measured absorption coefficient for an  $n$ -type sample of about 2 microns in thickness. A step can be seen at about 0.61 eV. The energy  $h\nu_2$  can be written:

$$h\nu_2 = E_G + \zeta + \frac{\hbar^2}{2m_2} k_\zeta^2,$$

where  $m_2$  is effective mass of the  $V_2$  band. The value of  $\zeta$  can be estimated from the carrier concentration. From measurements made on two samples with different electron concentrations,  $3.7 \times 10^{17} \text{ cm}^{-3}$  and  $6.6 \times 10^{17} \text{ cm}^{-3}$ , the values obtained for  $m_2/m$  are about 0.012.

The step in the absorption is small, corresponding to  $\Delta\alpha \sim 1000 \text{ cm}^{-1}$  as shown in Fig. 8. On the other hand,

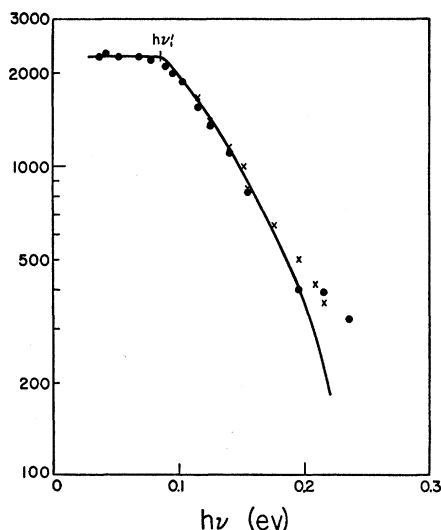


FIG. 9. Long wavelength absorption in degenerate *p*-type sample at  $\sim 5^\circ\text{K}$ . The points are measured on two samples of comparable carrier concentrations,  $\sim 5.5 \times 10^{17} \text{ cm}^{-3}$ . The curve is calculated for  $h\nu_{12}' = 0.085 \text{ eV}$ .

the absorption in *p*-type degenerate samples should be produced entirely by transitions from the  $V_2$  to the conduction band, at photon energies smaller than  $h\nu_1'$ . Curve A, Fig. 6 leads us to expect an absorption of about  $4000 \text{ cm}^{-1}$  to be associated with such transitions. The observed step in the absorption of *n*-type samples seems therefore to be too small. One possible explanation is that there are indirect transitions from  $V_1$  and  $V_2$  to the conduction band which would be included in the absorption given by curve A, Fig. 6. Another possibility is that the  $V_2$  band may also be warped, the consequence of which would be to spread out the absorption step and make it appear smaller.

It has been mentioned in connection with Fig. 1 that curve 5 for a degenerate sample at  $5^\circ\text{K}$  is not nearly as steep as expected. Since the edge corresponds to the threshold of transitions from  $V_1$  to the conduction band, the warping of  $V_1$  band and consequent difference between  $h\nu_1$  and  $h\nu_1'$  is a cause for the edge to be less steep. Curve C, Fig. 1, is measured on a sample of  $2.3 \times 10^{18} \text{ cm}^{-3}$  electron concentration corresponding to  $k = 4.85 \times 10^6 \text{ cm}^{-3}$ . The difference between  $h\nu_1$  and  $h\nu_1'$  is  $(\hbar^2 k^2/2)(1/m_1' + 1/m_1)$ . Taking a reasonable value  $m_a = 0.18m$  and using the values of  $m_a/m_1'$  and  $m_a/m_1$  obtained before we get  $h\nu_1' - h\nu_1 = 0.062 \text{ eV}$ . The spread

of  $h\nu$  indicated by this difference is of the right order of magnitude to account for the slope of curve C.

#### LONG WAVELENGTH ABSORPTION IN *P*-TYPE SAMPLES

The absorption at small photon energies, seen in Fig. 3, is apparently produced by hole transitions between valence bands  $V_1$  and  $V_2$ , like in the case of *p*-type germanium<sup>20</sup> indium arsenide<sup>21</sup> and gallium arsenide.<sup>22</sup> For a *p*-type degenerate sample at low temperature, a sharp high-frequency cutoff would be expected for the absorption if both energy bands had spherical surfaces of constant energy. Estimate, similar to that given in connection with the absorption edge, shows that the falloff of the experimental curve is much too gradual to be accounted for by the straggling of hole distribution at the Fermi level. The warping of the  $V_1$  band would lead to a gradual decrease absorption between  $h\nu_{12}'$  and  $h\nu_{12}$ . Figure 9 shows the long wavelength absorption measured on two samples of similar carrier concentrations. The absorption becomes constant toward small photon energies. Assuming that the absorption varies according to the hole occupation of the states in the  $V_1$  band we can calculate the drop of absorption beyond  $h\nu_{12}'$ . The curve in Fig. 8 is calculated for a value of  $h\nu_{12}'$  which seems to give the best fit with the experimental data. For the carrier concentration of the samples, the value of  $h\nu_{12}'$  used corresponds to an effective mass of  $0.014m$  for the  $V_2$  band. This value is in reasonable agreement with the value,  $0.012m$ , obtained from the study of *n*-type samples.

According to the interpretation, the value of  $h\nu_{12}'$  should increase as the square root of the hole concentration. Figure 3 shows that the absorption indeed falls off at higher  $h\nu$  for larger carrier concentration. However, we would also expect the absorption to be independent of carrier concentration for  $h\nu < h\nu_{12}'$ , whereas the observed absorption increases with carrier concentration even for small  $h\nu$ . This phenomenon indicates that the absorption may be associated with indirect rather than direct transitions. It remains to be seen whether the low-frequency absorption becomes a constant for smaller carrier concentrations. There is, however, a limit for the carrier concentration below which the sample will not remain degenerate at low temperature.

<sup>20</sup> W. Kaiser, R. J. Collins, and H. Y. Fan, Phys. Rev. **91**, 1380 (1953); H. B. Briggs and R. C. Fletcher, Phys. Rev. **91**, 1342 (1953).

<sup>21</sup> F. Matossi and F. Stern, Phys. Rev. **111**, 472 (1958).

<sup>22</sup> R. Braunstein, J. Phys. Chem. Solids **8**, 280 (1959).